

An Enhanced Projection Pursuit Tree Classifier with Visual Methods for Assessing Algorithmic Improvements

Natalia da Silva¹ Dianne Cook² Eun-Kyung Lee³

¹Instituto de Estadística (IESTA), Universidad de la República, Montevideo, Uruguay

²Department of Econometrics and Business Statistics, Monash University, Melbourne, Australia

³Department of Statistics, Ewha Womans University, Seoul, Republic of Korea

Abstract

This paper presents enhancements to the projection pursuit tree classifier and visual diagnostic methods for assessing their impact in high dimensions. The original algorithm uses linear combinations of variables in a tree structure where depth is constrained to be less than the number of classes—a limitation that proves too rigid for complex classification problems. Our extensions improve performance in multi-class settings with unequal variance-covariance structures and nonlinear class separations by allowing more splits and more flexible class groupings in the projection pursuit computation. Proposing algorithmic improvements is straightforward; demonstrating their actual utility is not. We therefore develop two visual diagnostic approaches to verify that the enhancements perform as intended. Using high-dimensional visualization

techniques, we examine model fits on benchmark datasets to assess whether the algorithm behaves as theorized. An interactive web application enables users to explore the behavior of both the original and enhanced classifiers under controlled scenarios. The enhancements are implemented in the R package `PPtreeExt`, which is available on CRAN.

Keywords: classification, heterogeneous variance, machine learning, projection pursuit, separability, tree classifier

1 Introduction

Loh (2014) provides an extensive overview of decades of research on classification and regression tree algorithms. Tree models are useful because they are simple, yet flexible, fast to compute, widely applicable, and interpretable. A main drawback, though, is that most available methods use splits along single variables, making separations on a combination of variables harder to capture. The reason is that it is a much harder problem to optimize the search for linear combinations, and thus, there is a lack of useful software that provides oblique splits.

One available method and software is the projection pursuit tree (PPtree) (Lee et al. 2013). It optimizes a projection pursuit (PP) index, for example, the LDA (Lee et al. 2005) or PDA (Lee and Cook 2010) index among others, based on class information to identify one-dimensional projections that best separate the groups at each node. The PPtree tree structure is simpler than classic methods like `rpart` (Therneau and Atkinson 2025), as it restricts

the tree depth to $G - 1$ (G is the number of classes). At each node, PPtree separates the data into two groups by first deciding which classes to group together; the data are split into left and right branches based on two group means. This produces a compact and interpretable tree implemented in the `PPtreeViz` R package (Lee 2018).

One of the main advantages of PPtree is its ability to leverage the correlation between predictor variables to improve class separation. In some scenarios, it has been shown to outperform other classifiers, including random forests (RF) (Breiman 2001). PP addresses a known limitation of the original RF algorithm. It included oblique projections, but because it is based on randomly generated splits was practically infeasible. It is an inefficient algorithm for finding useful oblique splits.

The compact nature of PPtree means that it fits simply and does not require pruning. The resulting one-dimensional projections can be used to make visualizations of group separations. However, there are limitations that reduce its effectiveness. In multiclass problems, due to the way classes are grouped, the prediction boundaries are often too close to one group, resulting in unnecessarily high error rates. This happens because grouping of classes likely produces unequal variance-covariances, making the pooled variance-covariance used by LDA inadequate. Secondly, when classes have non-elliptical variance-covariance, or have multiple clusters per class, the rigidity of the $(G-1)$ -node structure is not sufficiently flexible. The algorithm is modified to address these limitations in two ways: (1) improving prediction boundaries by modifying the choice of split points through class subsetting; and (2) increasing flexibility by allowing multiple splits per group.

Proposing enhancements to algorithms is easy, and theoretically, the modifications may

seem sensible. In practice, they may not work as one envisions. Thus, an important part of developing algorithm modifications is providing validation that they are doing what is expected, or not. This means going beyond predictive accuracy to understanding the resulting models. A second objective of this paper is to provide visual diagnostics for the algorithm changes. This is two-fold: a shiny (Chang et al. 2025) app and tours to view the fits in high dimensions. The app is available in the `PPtreeExt` package (da Silva et al. 2026) along with the implementation of the modified algorithm. It allows users to generate 2D data sets with different types of separations and compare the model fits for the modified and the original algorithm. This was an essential tool in constructing the new algorithm, because it provides a side-by-side visualization of prediction boundaries to identify data patterns in which the different methods perform better. The second visual diagnostic is to use tours available in the `tourr` package (Wickham et al. 2011) to examine the high-dimensional structure of data sets and the resulting model fits, where the modified algorithm outperforms other classifiers. This explains the performance comparison results and intuition for why the modified algorithm performs better.

The paper is organized as follows: Section 2 provides background on the original PPtree algorithm, including its structure and limitations. Section 3 describes the extensions to the algorithm. Section 4 contains the examples on visually and numerically digesting the enhanced algorithm's performance. Finally, Section 5 discusses the changes, results of the comparison, and potential future directions.

2 Background to PPtree

Figure 1 illustrates the original PPtree algorithm for $G = 3$. Starting from the optimal projection, the left-side, most distant, cluster (green circles) is relabeled as g_1^* , while the other two clusters are combined and relabeled as g_2^* . A second projection vector is then computed using all observations, following the same procedure applied to these two new super-groups. A split point is determined using one of the predefined rules, and observations are assigned to branches by comparing their projected values to the cutoff.

The algorithm computes a split point using one of several methods, and the observations are allocated to groups based on whether their projected values fall below or above the cutoff. Since g_1^* contains only one of the original classes, the left branch becomes a terminal node. Because g_2^* still includes two original classes, the procedure is recursively repeated on the right branch.

There are eight different rules available for computing the split point on a given projection. Let $\bar{\mathbf{x}}_g$, \mathbf{x}_g^{med} , s_g , IQR_g , and n_g denote the mean, median, standard deviation, interquartile range, and sample size of group g , respectively. Table 1 summarizes the formulas used to calculate the split point value, c , under each rule.

Table 1: Rules for computing the split value, c , between two groups, on a data projection, using means, weighted mean, medians, standard deviations, and interquartile ranges.

Rule	Name	Formula
1	mean	$c = \frac{1}{2}\bar{\mathbf{x}}_1 + \frac{1}{2}\bar{\mathbf{x}}_2$
2	sample size weighted mean	$c = \left(\frac{n_2}{n_1+n_2}\right)\bar{\mathbf{x}}_1 + \left(\frac{n_1}{n_1+n_2}\right)\bar{\mathbf{x}}_2$
3	standard deviation weighted mean	$c = \left(\frac{s_2}{s_1+s_2}\right)\bar{\mathbf{x}}_1 + \left(\frac{s_1}{s_1+s_2}\right)\bar{\mathbf{x}}_2$

Rule	Name	Formula
4	standard error weighted mean	$c = \frac{s_2/\sqrt{n_2}}{s_1/\sqrt{n_1}+s_2/\sqrt{n_2}}\bar{\mathbf{x}}_1 + \frac{s_1/\sqrt{n_1}}{s_1/\sqrt{n_1}+s_2/\sqrt{n_2}}\bar{\mathbf{x}}_2$
5	median	$c = \frac{1}{2}med_1 + \frac{1}{2}med_2$
6	sample size weighted median	$c = \frac{n_2}{n_1+n_2}med_1 + \frac{n_1}{n_1+n_2}med_2$
7	IQR weighted median	$c = \frac{IQR_2}{IQR_1+IQR_2}med_1 + \frac{IQR_1}{IQR_1+IQR_2}med_2$
8	sample size and IQR weighted median	$c = \frac{IQR_2/\sqrt{n_2}}{IQR_1/\sqrt{n_1}+IQR_2/\sqrt{n_2}}med_1 + \frac{IQR_1/\sqrt{n_1}}{IQR_1/\sqrt{n_1}+IQR_2/\sqrt{n_2}}med_2$

2.1 Algorithm

The PPtree algorithm (Lee et al. 2013) follows a multi-step procedure to identify linear combinations of predictors that optimally separate classes in multi-class settings. Let $d_n = \{(\mathbf{x}_i, y_i)\}_{i=1}^n$ denote the dataset, where \mathbf{x}_i is a p -dimensional vector of explanatory variables. The corresponding class label is $y_i \in \mathcal{G}$, with $\mathcal{G} = \{1, 2, \dots, G\}$, for $i = 1, \dots, n$. The construction of a PPtree classifier follows a four-step algorithm, as follows:

Input: Dataset $d_n = \{(\mathbf{x}_i, y_i)\}_{i=1}^n$, with $\mathbf{x}_i \in \mathbb{R}^p$, $y_i \in \mathcal{G} = \{1, \dots, G\}$

Output: A projection pursuit classification tree with at most $G - 1$ internal nodes

- **Step 1: Class Separation.** Optimize a PP index (e.g., LDA or PDA) to find a projection vector α that best separates all classes in the current node.
- **Step 2: Binary Relabeling.** On projected data, $z_i = \alpha^T \mathbf{x}_i$, compute projected class means $\bar{z}_1, \dots, \bar{z}_G$. Identify the pair with the largest mean difference and compute the midpoint mp . Relabel the observations into two super-classes, g_1^* and g_2^* , depending on whether \bar{z}_g is smaller than the midpoint mp .

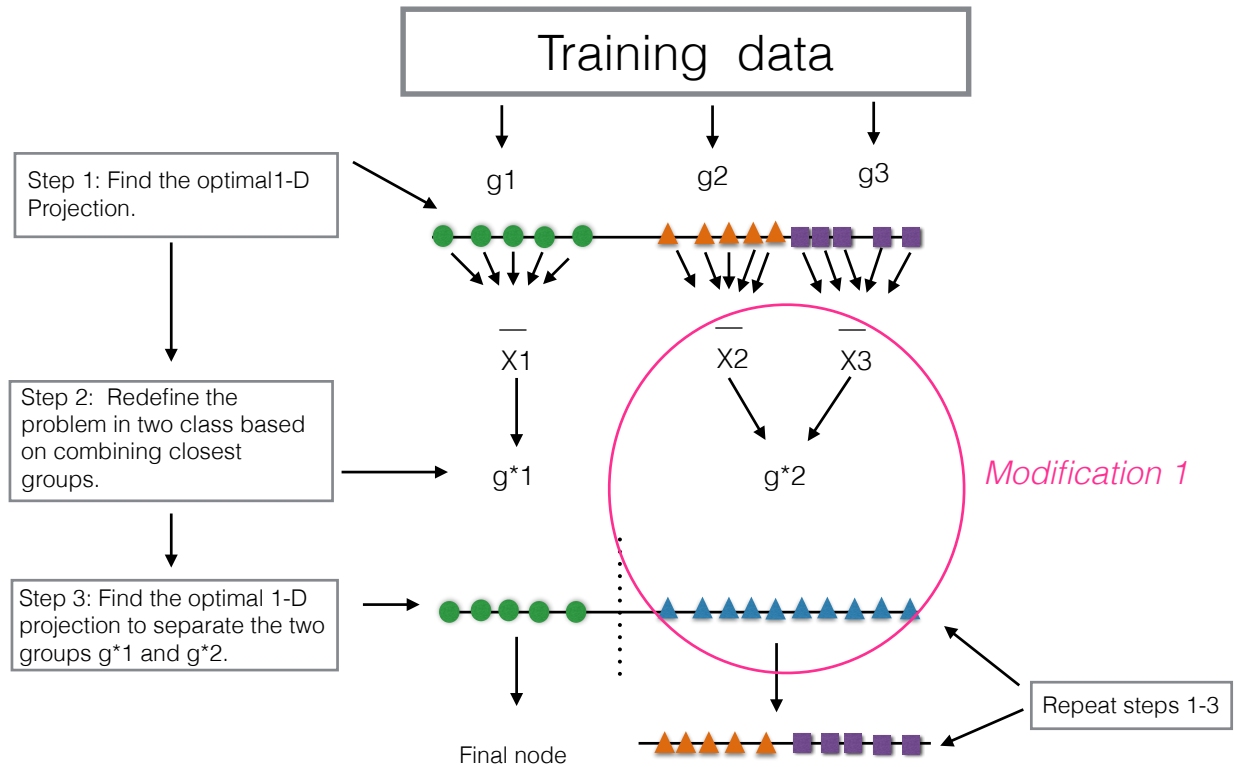


Figure 1: Illustration of the original PPtree algorithm for $G = 3$. In step 1, PP optimization decides on the best linear projection. Step 2 combines two groups to make a two-group classification. The PP optimization is computed for two group problem, and an appropriate split is decided. This is repeated for the remaining two groups to get the final model containing two splits. The locations where modifications will be made are circled.

- **Step 3: Node Splitting.** Optimize a new projection α^* to separate g_1^* and g_2^* based on the relabeled classes. Define the split value c on $z_i^* = \alpha^{*T} \mathbf{x}_{g_i^*}$ using a predefined rule (e.g., mean or weighted mean). Split the node using the rule $z_i^* < c$.
- **Step 4: Recursive Partitioning.** Repeat Steps 1–3 for each child node until every terminal node contains only one original class.

2.2 Less desirable aspects

The decision boundaries of a classifier reflect how the model partitions the feature space and adapts to class separations. Visualizing the decision boundaries provides valuable insights into model behavior and limitations. To illustrate the PPtree algorithm relative to the classical `rpart` and the motivation for improving PPtree, we use two simulated three-class 2D data sets. Data set `LC` has separations on linear combinations of variables (Figure 2), and data set `MC` has multiple clusters in a class (Figure 3). The three classes are indicated by squares (S, violet), circles (C, green), and triangles (T, orange).

Figure 2 shows the decision boundaries produced by `rpart` (left) and `PPtree` (right), and percentage error, for the `LC` data. The class clusters are best separated using linear combinations of the two variables. The `rpart` algorithm, which relies on axis-aligned splits, must approximate the ideal boundary using rectangular steps. Even with many steps, it cannot be as efficient as the oblique splits provided by `PPtree`. The two steps of `PPtree` are to split the S cluster (violet) first, and then split C (green) and T (orange). Although the group structure is similar across the three classes, the resulting decision boundaries are not parallel. This occurs because the initial split uses the combined information from the C and

T clusters - treated as a super class - to compute the projection and determine the splitting point. This also results in the boundary between T and S being too close to T. Alternative rules for computing the split value (see Table 1) can impact the position and orientation of these decision boundaries, but in this case does not fix the deficiency.

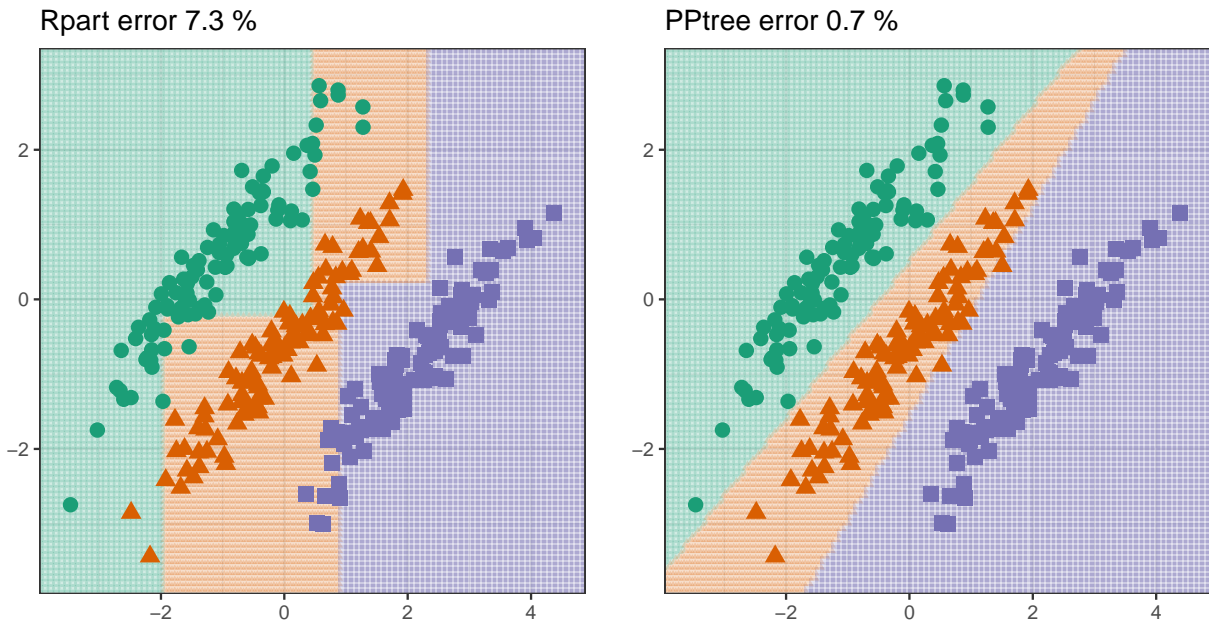


Figure 2: Comparison of decision boundaries produced by the `rpart` (left) and `PPtree` (right) algorithms on the LC data. The boundaries generated by `PPtree` are oblique to the coordinate axes, appropriately capturing the separations as linear combinations of the two variables. Even with many splits, the `rpart` algorithm cannot elegantly classify this data.

Figure 3 compares the `rpart` and `PPtree` decision boundaries for the data set MC, where class T has two separated clusters. It highlights the limited flexibility of the decision boundaries produced by `PPtree`. In this scenario, the T cannot be separated using a single linear partition, and `PPtree` fails to capture it because the tree depth is limited to a single terminal node for each class. In contrast, the more traditional `rpart` algorithm performs better in

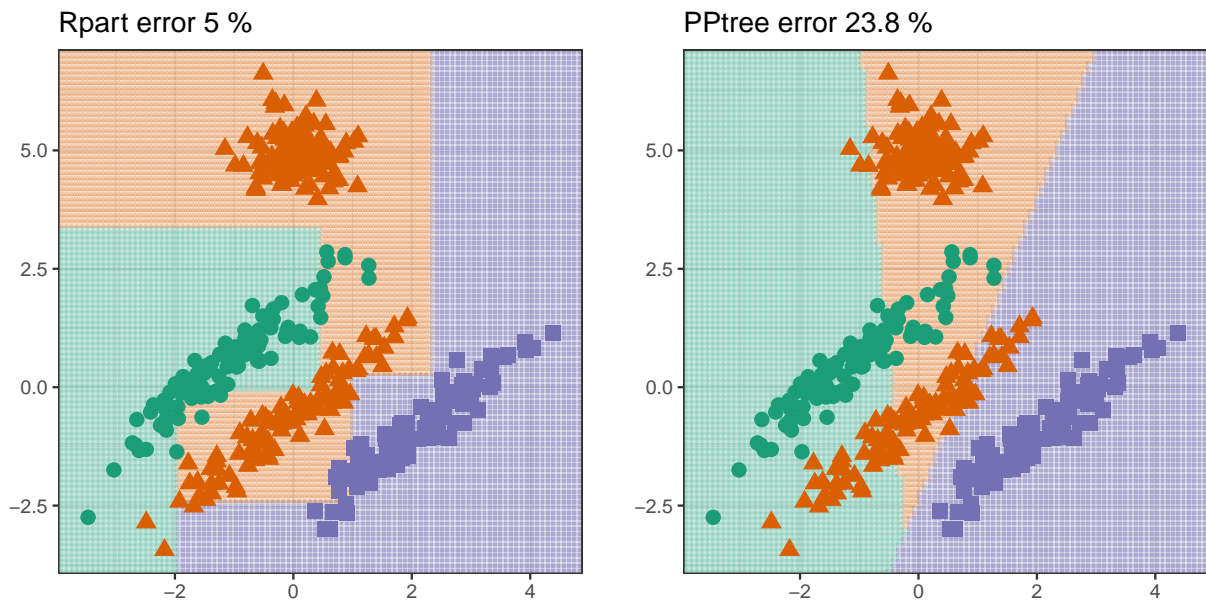


Figure 3: Comparison of decision boundaries produced by the `rpart` (left) and `PPtree` (right) algorithms on the MC data. The T class (orange triangles) cannot be separated using a single linear partition, and `PPtree` fails to model it accurately because each class must be assigned to a single terminal node. This illustrates the need for allowing more splits in `PPtree` to capture unusually shaped clusters and separations involving combinations of variables.

this case, as its recursive structure allows it to accommodate the relatively simple non-linear separation. However, `rpart` fails to capture the separation between classes as linear combinations. This shows why more splits should be allowed for the PPtree algorithm.

3 PPtree extensions

The algorithm has been extended in two main ways, as indicated by the annotation in Figure 1. Section 4.1 explains how we can compare the changes these modifications induce on the boundaries relative to `rpart` and PPtree using the Shiny app.

3.1 Modification 1: Subsetting classes to produce better boundaries

The first modification targets the re-grouping step of the original algorithm. Rather than combining all remaining classes into a single super-class, only the two closest ones, as identified by the smallest difference in their projected means, are used to compute the next projection and define the split point. This step is now as follows:

- **Step 2*: Binary Relabeling.** Find an optimal one-dimensional projection α^{**} , using a subset of $\{(\mathbf{x}_i, y_i^*)\}_{i=1}^n$ to separate the two class problem g_1^* and g_2^* . To this second projection **only information from the two closest groups**, one from g_1^* and the other from g_2^* are used. The best separation of g_1^* and g_2^* is determined by $\alpha^{*T} \bar{\mathbf{x}}_{g_1^*} < c$; then g_1^* is assigned to the left node else assign g_2^* to the right node, where $\bar{\mathbf{x}}_{g_1^*}$ is the mean of g_1^* .

In Figure 1 this would correspond to dropping class g_3 from the current node. The projection is then computed using only classes g_1 and g_2 (reabeled as g_1^* and g_2^*). The choice of the existing eight available rules is then applied to determine the optimal split point, to create the terminal node for g_1 . Subsequently, class g_3 is reintroduced, and a new projection is computed to best separate it from g_2 . The split is made on this set of observations, creating two more terminal nodes, completing the tree construction.

3.2 Modification 2: Multiple splits per class based on entropy reduction

To allow for multiple splits, various changes are needed: the split is made on the optimal projection, not after groups are combined, and new stopping rules are defined to prevent over-fitting. Figure 4 illustrates the change to the algorithm for this modification.

In PPtree, the decision boundary split is made using the means for the two groups, just like is done with linear discriminant analysis. This modification changes this to follow the `rpart` algorithm, minimizing entropy, with the difference being that it is done on the optimal 1-D projected data. That is, the modification computes the negative entropy criteria:

$$E(s) = - \sum_{j=1}^G p_{js} \log(p_{js}) \quad (1)$$

where p_{js} is the proportion of observations from class j in subset s , and G is the number of classes. Lower values of $E(s)$ indicate purity, reaching zero when all observations in the subset belong to the same class. The impurity value for a split is calculated by combining

the values of the left and right subsets:

$$E(s_L, s_R) = \frac{n_L}{n_L + n_R} E(s_L) + \frac{n_R}{n_L + n_R} E(s_R) \quad (2)$$

where n_L, n_R are the number of observations in the left and right subsets, respectively. Across all possible splits, the lowest combined impurity, $E(s_L, s_R)$, is computed for all possible split points, defined as the midpoints between consecutive ordered projected values, denoted $\mathcal{C} = \{c_1, \dots, c_{n_L+n_R-1}\}$. The split point that minimizes the combined entropy is selected:

$$\min_{c \in \mathcal{C}} E_c(s_L, s_R)$$

.

In addition, three stopping rules are introduced, which are similar to `rpart`: the node is pure, there are fewer than a specified number of observations in the node, or the reduction in impurity is less than a specified tolerance value. These changes provide the modified algorithm to be:

Input: Dataset $d_n = \{(\mathbf{x}_i, y_i)\}_{i=1}^n$, with $\mathbf{x}_i \in \mathbb{R}^p$, $y_i \in \mathcal{G} = \{1, \dots, G\}$

Output: A projection pursuit classification tree with entropy-based node splitting

- **Step 1: Class Separation.** Optimize a PP index (e.g., LDA or PDA) to find a projection vector α that best separates the classes in the current node.
- **Step 2: Projection and Candidate Splits.** On the projected data, $z_i = \alpha^T \mathbf{x}_i$, define candidate splits as midpoints between consecutive z_i values.

- **Step 3: Impurity Evaluation.** For each candidate split c , divide the data into $s_L = \{z_i < c\}$ and $s_R = \{z_i \geq c\}$. Compute the class proportions p_{js} for each subset and evaluate the entropy:

$$E(s) = - \sum_{j=1}^G p_{js} \log(p_{js})$$

Compute the total impurity as:

$$E(s_L, s_R) = \frac{n_L}{n_L + n_R} E(s_L) + \frac{n_R}{n_L + n_R} E(s_R)$$

- **Step 4: Best Split Selection.** Select the split point c^* that minimizes $E(s_L, s_R)$. Split the node using the rule $z_i < c^*$.
- **Step 5: Recursive Partitioning.** Repeat Steps 1–4 recursively on each child node until some of the following stopping criteria are met:
 - All observations in the node belong to the same class;
 - The node size is smaller than a minimum threshold n_s ;
 - The entropy reduction is smaller than a threshold ent_s .

4 Comparative performance

Three approaches are used to examine the effectiveness of the modifications. The first is a Shiny app which generates structures in 2-D and shows the model fits for three algorithms: `rpart`, `PPtree`, and the `PPtree` extensions. It was developed and used to decide on effective

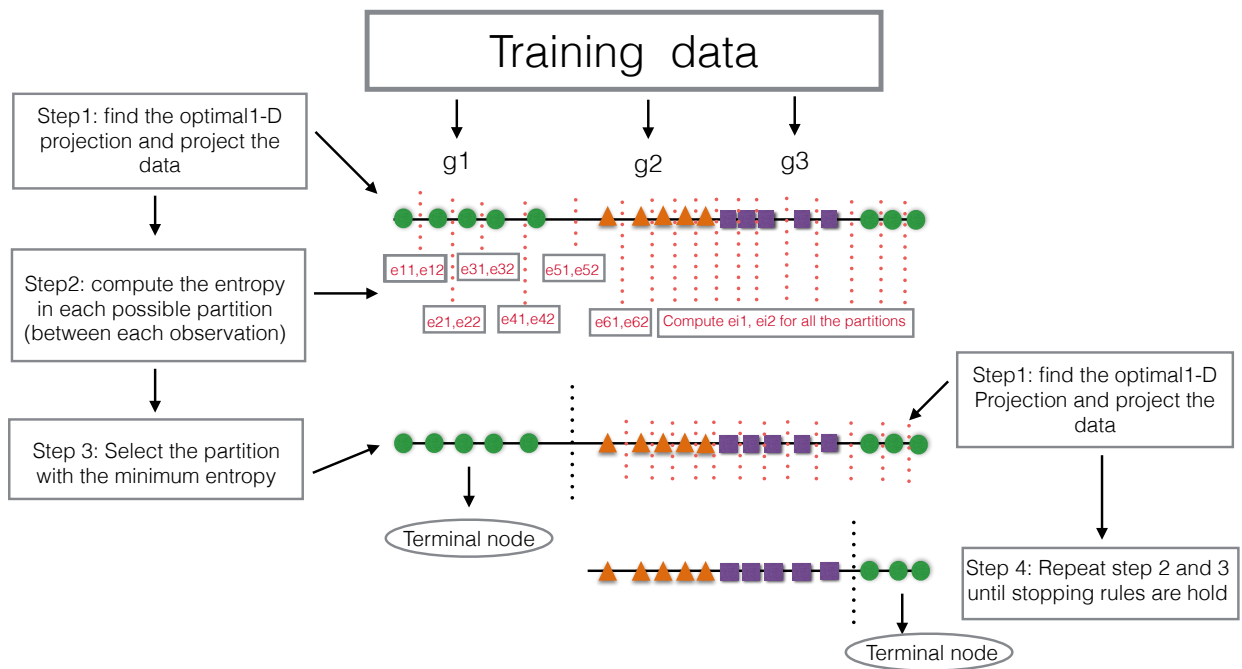


Figure 4: Illustration of the algorithm with modification 2 applied to a three-class problem. Projections of the data are computed at each node, and multiple splits per class are allowed. An impurity-based criterion, such as entropy, is used to determine when and how often to split observations within a node.

changes to the algorithm. The second is a simulation study on 94 benchmark data sets to compare test errors. Lastly, to understand where, why, and how the extensions work, we examine the data visually in high dimensions along with the fitted models.

4.1 Exploring the algorithm changes interactively

The Shiny app includes methods for simulating 2D classification problems, and displays the decision boundaries generated by three different algorithms: CART, PPTree, and the proposed extensions as implemented in the `rpart`, `PPTreeViz`, and `PPTreeExt` packages, respectively.

There are three data generation methods, “Basic-Sim”, “Sim-Outlier”, and “MixSim”. Basic-Sim simulates classes with separations between clusters on linear combinations of variables, by user-specified correlations between variables for each cluster. Sim-Outlier uses the same approach with the addition of a cluster of outliers corresponding to one of the classes. These two methods allow only for three-cluster data. The user can control the number of observations in each class, the class means, and the Sim-Outlier mean and shape of the outlier groups. MixSim uses a Gaussian mixture model using the `MixSim` package (Melnykov et al. 2012) to simulate class clusters, with any number of classes. While all classes have equal sample size, the user can choose this and also specify values for the `MixSim` algorithm. Figure 5, Figure 6, Figure 7 show the interface for the three different data-generating methods. Clicking “Ok” will simulate new samples.

The decision boundaries for `rpart`, `PPTree`, and the modified `PPTree` (implemented in `PPTreeExt`) are displayed side by side for visual comparison. The user can choose which

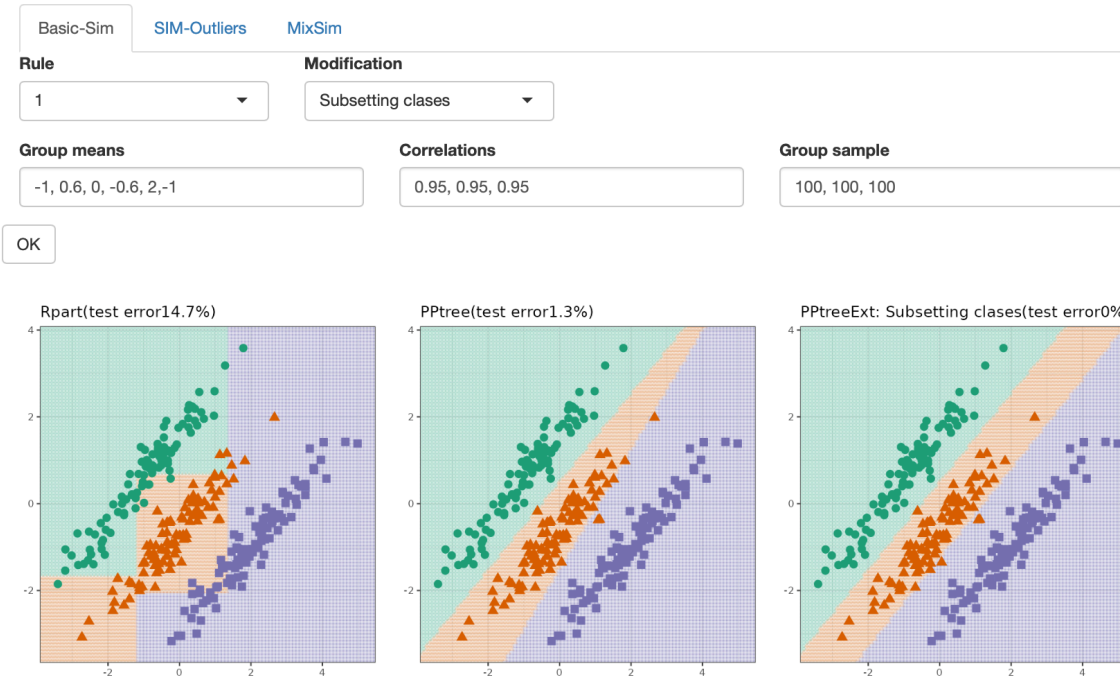


Figure 5: Comparing the fits for three-class data with a strong correlation between variables. Modification 1 (different subsetting rules) of **PPtree** is shown. The modification produces lower error and decision boundaries that are more symmetrically placed between the class clusters.

modifications of **PPtree** to show. For the other algorithms, only the default parameter choices are used.

In Figure 5, three-class data with a strong correlation between variables is simulated. Modification 1 (different subsetting rules) is applied, and rule 1 (Table 1) is used to compute the split point. The modified **PPtree** achieves an error rate comparable to the original **PPtree**, with both substantially outperforming **rpart**. The change in boundaries is subtle, but more satisfying. Between classes S (violet squares) and T (orange triangles), the boundary better matches the separation - it is not pulled away from this split by using LDA on the super-group (T and C).

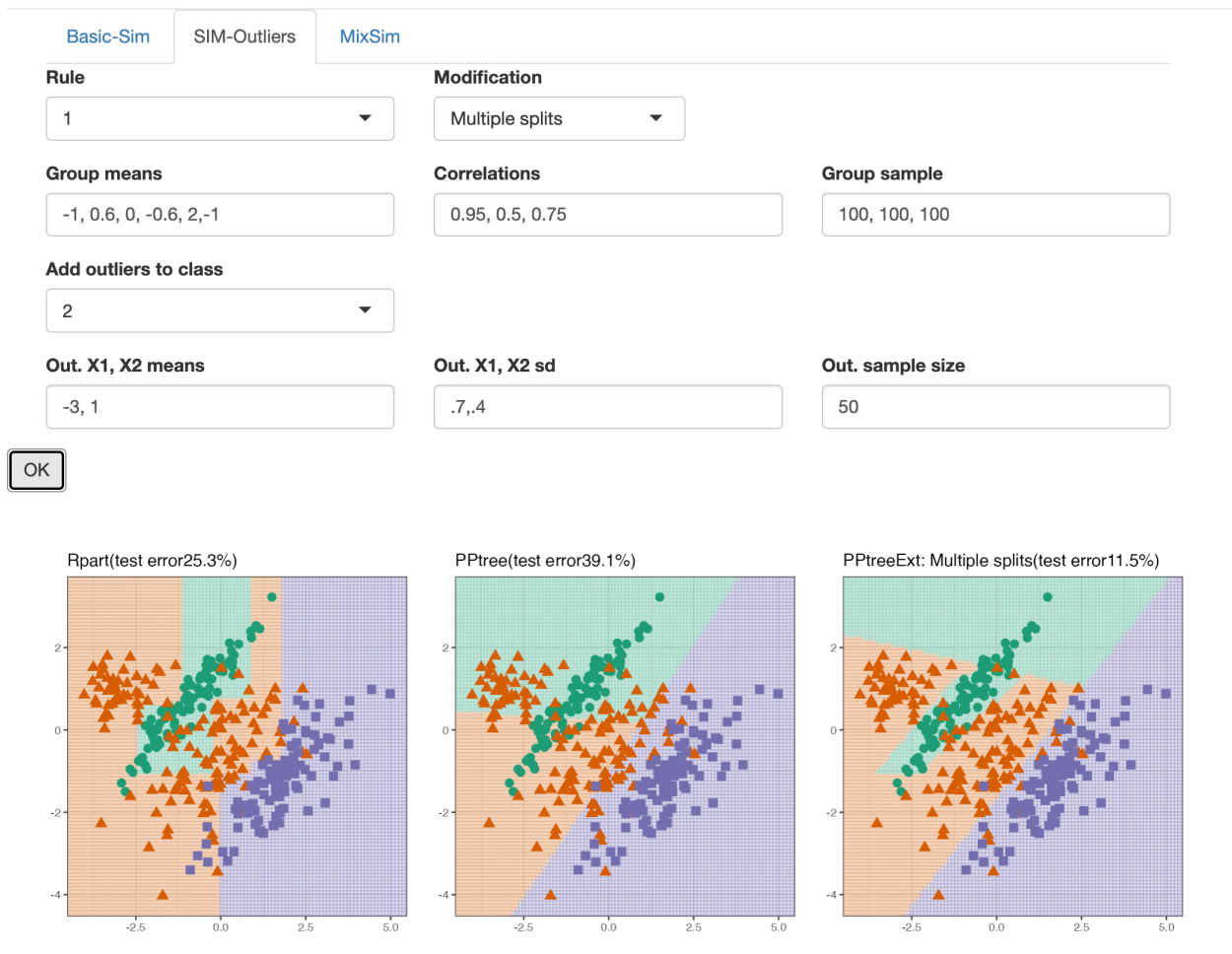


Figure 6: Comparing the fits for data where one class has two distinct clusters. Modification 2 (multiple splits) of `PPtree` is used. The modification produces lower error and better decision boundaries.

Figure 6 shows data where one class has two separated clusters, as simulated by `Sim-Outlier`. The `PPtree` extension used is modification 2 (multiple splits). It yields a substantial improvement over the other algorithms, both in lower error and more sensible boundaries. The use of multiple splits enables the small group of outliers from class T (orange triangles) to be better classified.

The data in Figure 7 has 5 clusters of different shapes. Modification 2 (multiple splits) is examined. Again, we see that the modified algorithm outperforms `PPtree` and `rpart`, in

both lower error and better boundaries.

The interactive application provides insight into how modifications to the algorithm affect model fit. Comparing the fitted models follows the principle of visualizing the model in the data space (Wickham et al. 2015). This app has been a valuable tool for debugging and evaluating the algorithmic behavior. By adjusting the simulated data and model parameters, it becomes evident that small changes in the data can result in substantial changes in the fitted model, particularly when projections are involved. By understanding the effect in 2-D, we aim to better understand how the algorithm might also behave in high-dimensional settings.

4.2 Numerical performance

We compare the predictive performance for the extended PPtree algorithm with several classification methods, CART, PPtree (LDA, PDA), random forest, PPforest, and SVM, using 94 benchmark data sets. (LDA indicates PP conducted with the linear discriminant index, and PDA indicates PP conducted using the penalized linear discriminant index.) Figure 8 summarizes the performance on data sets where the modified algorithm outperformed other tree methods, and [?@tbl-data-tab2](#) summarizes the main characteristics of each data set, including the number of observations, predictors, number of classes, class imbalance, and absolute average correlation among predictors. Imbalance quantifies the disparity in class sizes (0 indicates perfectly balanced classes, the biggest proportion size difference between classes), while higher correlation suggests a greater potential for class separation through linear combinations of variables. (The Appendix contains the links to the original data sources,

Basic-Sim SIM-Outliers MixSim

Rule

Modification

Sample size

BarOmega desired average overlap

MaxOmega desired maximum overlap

K number of components

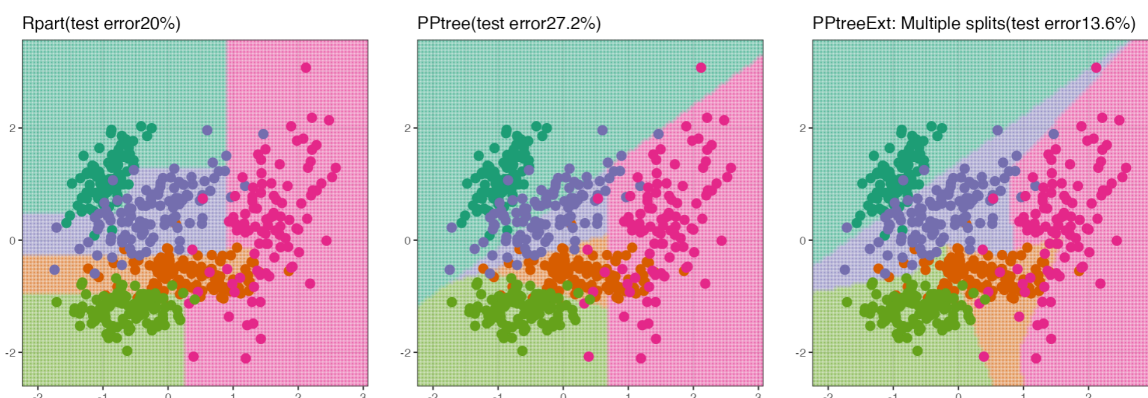


Figure 7: Comparing the fits for five-cluster Gaussian mixtures. Modification 2 of PPtree is used. This produces lower error and reasonable decision boundaries.

full performance, and data set summaries.)

In the simulation, two-thirds of the observations in each data set are randomly selected for training (using stratified sampling), and the remaining one-third is used for testing and computing the prediction error. This process is repeated 200 times to assess the variance in performance.

Figure 8 summarises the performance for the 18 data sets, where PPtreeExt with modification 2 outperforms the other tree algorithms. In three of these data sets, it also has the lowest error than the ensemble-based classifiers, also. The plots are ordered according to

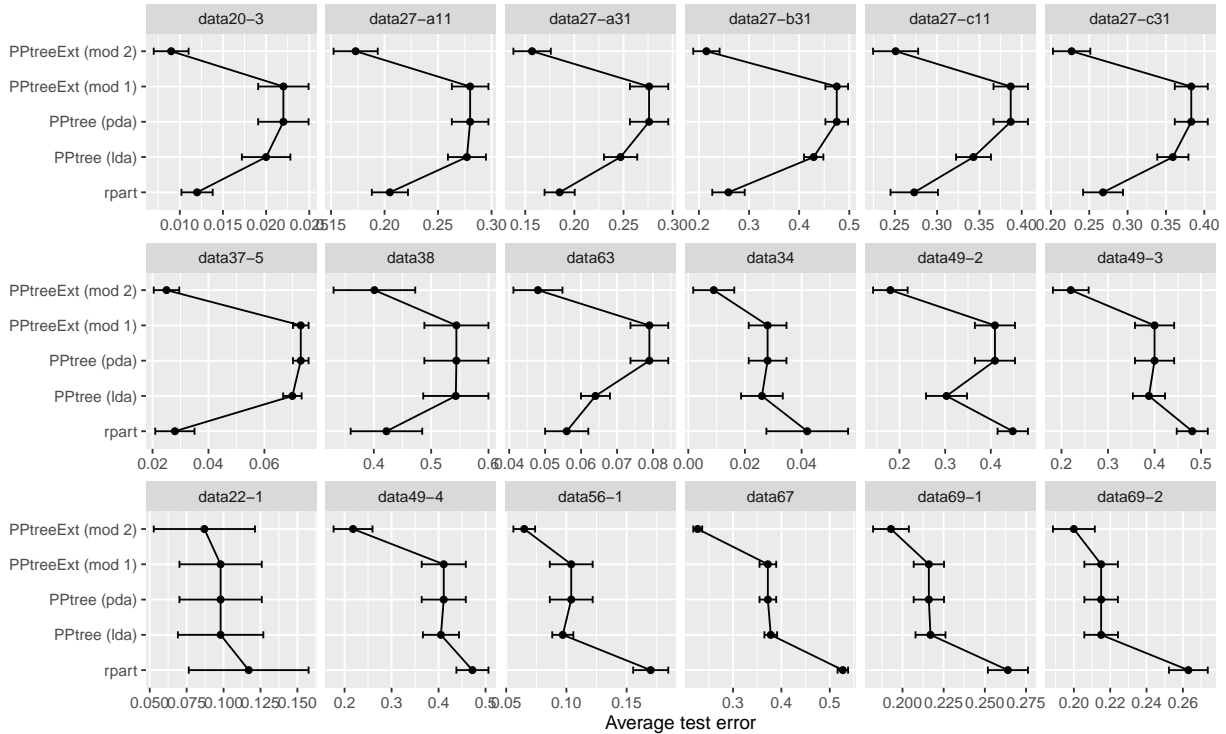


Figure 8: Average test error with 95% error bars from 200 training/test splits of benchmark data for four models: `rpart`, `PPtree`, `PPtreeExt` modifications 1 and 2, where the latter performs better than the others. The order of the plots is based on the pattern of errors: at top left `PPtreeExt (mod 2)` is best but only slightly better than `rpart`, and at bottom right each of the `PPtree` versions iteratively performs better than `rpart`.

the pattern of test error. In data sets `data20-3`, `data27-a11`, `data27-a31`, `data27-b31`, `data27-c11`, `data27-c31`, `data37-5`, `data38`, and `data63`, only `PPtreeExt (mod 2)` outperforms `rpart`. For `data34` and `data49-2` results are mixed. For the other data sets (`data49-3`, `data22-1`, `data49-4`, `data56-1`, `data67`, `data69-1`, `data69-2`), each of the methods does better than `rpart`. The variability across training and test splits is high for some data sets (`data38`, `data22-1`). Data sets `data20-3`, `data49-2`, and `data69-1`, representing a range of numerical performance, are chosen to investigate why `PPtreeExt` performs better, using high-dimensional visualisation in the next section.

Table 2: Overview of benchmark datasets where the proposed tree-based extensions outperform the selected tree methods. The table summarizes the number of observations, predictors, number of classes, class imbalance, and absolute average correlation among predictors. Imbalance quantifies the disparity in class sizes (0 indicates perfectly balanced classes), while higher correlation suggests a greater potential for class separation through linear combinations of variables.

dataset	Cases	Predictors	Groups	Imbalance	Correlation
data20-3	8143	5	2	0.58	0.45
data27-a11	1747	18	5	0.38	0.24
data27-a31	1834	18	5	0.28	0.27
data27-b31	1424	18	5	0.21	0.24
data27-c11	1111	18	5	0.14	0.27
data27-c31	1448	18	5	0.17	0.27
data37-5	17560	53	5	0.21	0.16
data38	182	12	2	0.43	0.21
data63	6598	166	2	0.69	0.27
data34	1372	4	2	0.11	0.43
data49-2	606	100	2	0.03	1.00
data49-3	606	100	2	0.01	0.99
data22-1	258	5	4	0.25	0.12
data49-4	606	100	2	0.01	0.99
data56-1	7494	16	10	0.01	0.27
data67	20000	16	26	0.00	0.18
data69-1	5000	21	3	0.01	0.30
data69-2	5000	40	3	0.01	0.09

4.3 Visual explanations of performance

Exploring high dimensions is tricky, so it is helpful to set some objectives before leaping into the vast space. We would expect the modified PPtree algorithm to

- outperform `rpart` when the best separation between groups is in oblique directions
- and outperform PPtree when class variances are different, or when there are multiple clusters for any class.

This can be investigated visually using a tour. There are several strategies to use for ap-

proaching this:

1. On the data
 - a. Work on two groups at a time, if there are more than 2
 - b. Use a guided tour on the data to find the combinations of the variables where the groups are separated
2. Predict a grid of values that covers the data domain, for the methods interested in comparing, `PPtreeExt`, `rpart`, and `PPtree`, as can be done using the `classifly` package (Wickham 2022), and then
 - a. subset to the points near the border generated by the classifier.
 - b. record a sequence of projection bases that shows the boundary created by the method in focus.
 - c. use the same projection sequence to view the boundaries for the three different methods, and possibly use a slice tour to focus on the boundary near the center of the data domain.

Figure 9 shows two projections of the `data20-3` illustrating why `PPtreeExt` performs better. The projections are 2-D from the full 5-D space. Color indicates the two classes (0 is blue and 1 is red). The circles represent the projection coefficients. Using a clock dial analogy, in the first projection (a), `V3` is pointing towards 1 o'clock, and `V4` is pointing towards 10. `V2` is also pointing to 1, but is very small. The difference in the two groups is in the direction of 1, so `V3` is likely mostly contributing to this, with a small contribution from `V2`. In the second projection (b) `V3` points to 5, `V4` points to 2, `V5` points to 3, and `V2` points to 9. The separation is in the direction of 5 o'clock, suggesting again that `V3` is primarily important.

Group 0 is split on either side of group 1, which means that the PPtree algorithm would not be able to capture both clusters, but modification 2 would. The separation between the two classes is mostly on V3 but small contributions from other variables help to improve the separation. This means that `rpart` will not work quite as well because it will focus on splitting V3, ignoring the other variables.

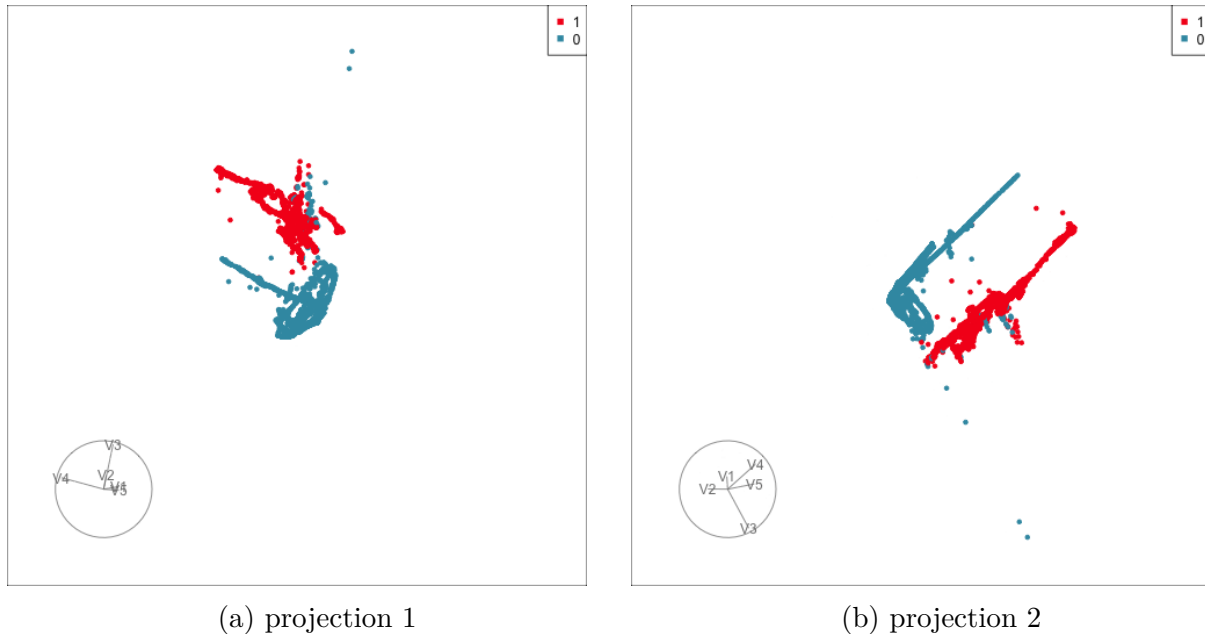


Figure 9: Two projections from a grand tour of data20-3, from which we can see why the `PPtreeExt` method is the most effective. Class 0 is split into two clusters on either side of group 1, which means that the original algorithm is not optimal. Secondly, the separation between the two groups is primarily V3 with small contributions from other variables, which gives `PPtreeExt` a slight edge over `rpart`.

From Figure 8, for data49-2, we can see that the original PPtree (with LDA) algorithm performs much better than a tree, and the `PPtreeExt` performs much better again. This data has 100 predictors and 2 classes (Table 2), which makes visualising more challenging than data20-3. A useful approach is to pre-process using principal component analysis (PCA) on the predictors, to reduce the number of variables to visualise, while maintaining class structure. In Figure 10 plot (a) shows PC 1 vs PC2, with points coloured by the two

classes. PC 1 explains 99.8% of the variability in the predictors, but it explains nothing of the class structure. This is not uncommon for PCA, where an interesting structure can be found in the smaller components. Plot (b) shows PC 2 vs PC 3, and here we see interesting class differences. Each class appears to have three linear pieces pointing in different directions. This supports why `PPtreeExt` might work well: in the combination of variables, the classes are nearly separable with multiple linear cuts. It's not feasible to continue working through principal components to tease apart the cluster structure relating to classes, so a good next step is to do PP with the guided tour. The optimal projection is shown in plot (c). It is computed on 26 PCs, and many of these contribute to this projection as seen by the mess of lines inside the circle representing the axes. The two classes are mostly linearly separable in this projection, but there is no clear gap between the clusters. The linear combination with so many variables is what causes some difficulties for a simple tree algorithm. The interesting shapes of the clusters for each class, which appear to be multiple linear pieces, mean that the `PPtreeExt` can find better separations than `PPtree`.

From Figure 8 we see that all of the `PPtree` versions perform better than an `rpart` fit on `data69-1`. This data has 21 predictors and 3 classes (Table 2). This is a sufficiently small-scale problem to examine using a tour, and we initially use a guided tour with the LDA index. This produced the projection shown in plot (a), where we see the primary difference between the three classes. These are each similar size, but oriented in such a way that in this 2-D projection, they form a triangle. Plots (b) and (c) show the boundaries using a slice tour with the same projection as used in (a) for `PPtreeExt` and `rpart`, respectively. This uses approach 2 above: created by predicting the class of points randomly generated from a

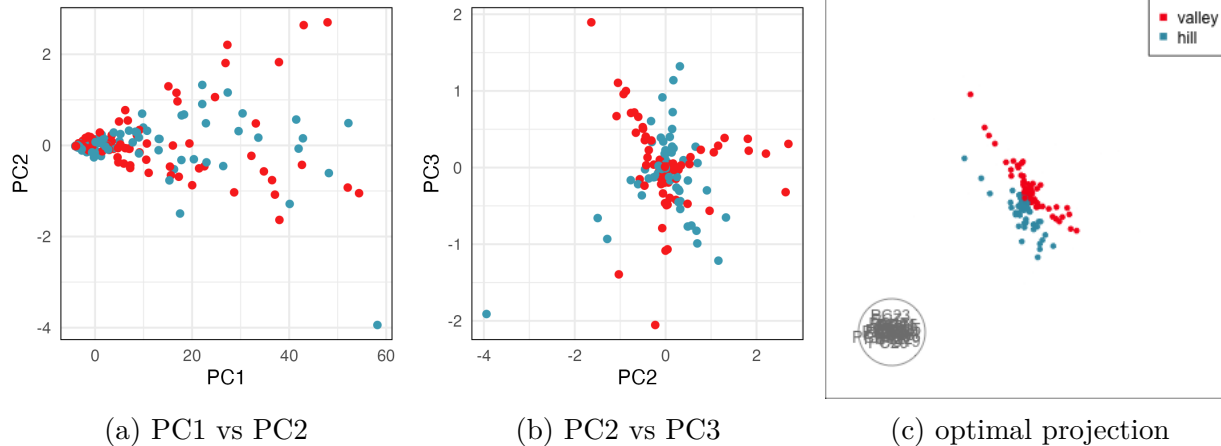


Figure 10: Examining why `data49-2` is best classified using `PPtreeExt`. Because there are 100 predictors, for visualisation it is useful to reduce the dimension using principal component analysis, and then examine the separation between groups. PC1 explains 99.8% of the overall variability among predictors, but it is not useful for separating the classes (a). PC2 and PC3 (b) have an interesting difference between the two classes, which shows why multiple linear splits might be useful. A guided projection pursuit tour on the first 26 principal components (c) shows that these classes could be separated with a linear combination. This is why the original `PPtree` classifier does better than the tree algorithm and also why the extension improves the performance.

uniform distribution in a 21-D cube of the same range as the data. The slice cuts through to the center of the box. We can see that `PPtreeExt` essentially fits the data shape neatly, but the `rpart` boundary is very messy. This data needs oblique cuts, which `PPtreeExt` provides but `rpart` does not. The modified algorithm handles the variance differences better than the original `PPtree`.

5 Discussion

This article has presented two modifications to the `PPtree` algorithm for classification problems implemented in the R package `PPtreeExt`. These changes result in a more flexible classification method that leverages linear combinations of variables. The performance study showed that the predictive performance of `PPtreeExt` with modification 2 is better than

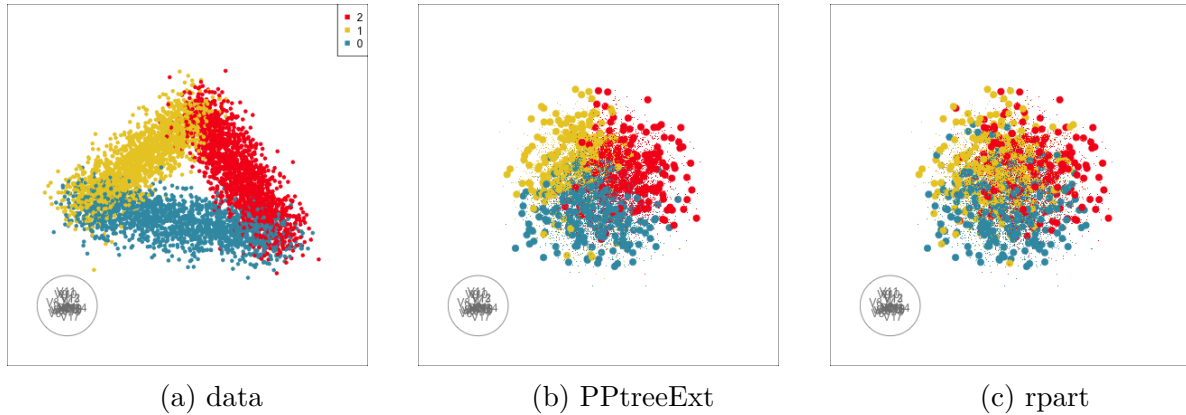


Figure 11: Examining why `data69-1` is best classified using `PPtreeExt`: (a) best projection from a guided tour shows that the data has three similar linear pieces oriented to form a triangle, (b) boundary produced by the `PPtreeExt` (mod 2) fitted model, and (c) boundary produced by `rpart` fitted model. The same projection is used in all plots to allow comparison. The boundary is examined by predicting the class of a uniform random sample of points in the data space, and viewed using a slice tour. The boundary for `PPtreeExt` (mod 2) mirrors what we learn from the data, that it is carving the data space into three equiangular chunks, but `rpart` is not capturing these linear combinations.

CART and PPtree in 18 out of 94 data sets. A web app was developed and shared to help understand and debug modifications to the algorithm.

Interpretability is increasingly important because predictions from algorithms may need to be defended in practice. We have shown how to examine the data and the fitted model using high-dimensional visual methods to understand why the PPtree extension performs better than other tree methods on some data sets. This approach is generally useful for assessing and diagnosing model fits.

Ultimately, this may provide better building blocks for a projection pursuit-based classification random forest algorithm (da Silva et al. 2021) as available in the `PPforest` R package (da Silva et al. 2025). The modified tree algorithm can be incorporated into a projection pursuit forest classifier (da Silva et al. 2025). Given its implicit variable selection mechanism, the ensemble is expected to handle nuisance variables more effectively than a single

tree. Using the PDA index (penalised discriminant analysis) also helps when there are many variables. Additionally, the use of bagging should yield improved and more robust performance in problems with nonlinear decision boundaries. This can be accomplished using the current PPforest package.

6 Supplementary Materials

This article was written in Quarto (Allaire et al. 2024), using the R package `ggplot2` (Wickham 2016) for visualizations. The files to reproduce the article and results are available at https://github.com/natydasilva/PPtreeExt_paper_JCGS. Animated gifs corresponding to Figure 9, Figure 10 and Figure 11 are in the `gifs` folder. The `code` directory contains the scripts for the simulations and to explore the model fits in high dimensions.

The `PPtreeExt` package provides the modified PPtree algorithm. The Shiny app is available at <https://natyds.shinyapps.io/explorapp/> and the app code is provided in the `PPtreeExt` package, so that it can be used locally for new algorithm developments.

- Allaire, J. J., Teague, C., Scheidegger, C., Xie, Y., and Dervieux, C. (2024), “Quarto.” <https://doi.org/10.5281/zenodo.5960048>.
- Breiman, L. (2001), “Random Forests,” *Machine learning*, Springer, 45, 5–32.
- Chang, W., Cheng, J., Allaire, J., Sievert, C., Schloerke, B., Xie, Y., Allen, J., McPherson, J., Dipert, A., and Borges, B. (2025), *Shiny: Web Application Framework for R*. <https://doi.org/10.32614/CRAN.package.shiny>.
- da Silva, N., Cook, D., and Lee, E.-K. (2021), “A Projection Pursuit Forest Algorithm for Supervised Classification,” *Journal of Computational and Graphical Statistics*, Taylor & Francis, 30, 1168–1180. <https://doi.org/10.1080/10618600.2020.1870480>.
- da Silva, N., Cook, D., and Lee, E.-K. (2025), *PPforest: Projection pursuit classification forest*. <https://doi.org/10.32614/CRAN.package.PPforest>.
- da Silva, N., Cook, D., and Lee, E.-K. (2026), *PPtreeExt: Projection Pursuit Classification Tree Extensions*. <https://doi.org/10.32614/CRAN.package.PPtreeExt>.
- Lee, E.-K. (2018), “PPtreeViz: An R Package for Visualizing Projection Pursuit Classification Trees,” *Journal of Statistical Software*, 83, 1–30. <https://doi.org/10.18637/jss.v083.i08>.
- Lee, E.-K., and Cook, D. (2010), “A Projection Pursuit Index for Large p Small n Data,” *Statistics and Computing*, Springer, 20, 381–392. <https://doi.org/10.1007/s11222-009-9131-1>.
- Lee, E.-K., Cook, D., Klinke, S., and Lumley, T. (2005), “Projection Pursuit for Exploratory Supervised Classification,” *Journal of Computational and Graphical Statistics*, Taylor & Francis, 14, 831–846. <https://doi.org/10.1198/106186005X77702>.
- Lee, Y. D., Cook, D., Park, J., and Lee, E.-K. (2013), “PPtree: Projection Pursuit Clas-

- sification Tree,” *Electronic Journal of Statistics*, Institute of Mathematical Statistics, 7, 1369–1386. <https://doi.org/10.1214/13-EJS810>.
- Loh, W.-Y. (2014), “Fifty Years of Classification and Regression Trees,” *International Statistical Review*, Wiley Online Library, 82, 329–348. <https://doi.org/10.1111/insr.12016>.
- Melnykov, V., Chen, W.-C., and Maitra, R. (2012), “MixSim: An R Package for Simulating Data to Study Performance of Clustering Algorithms,” *Journal of Statistical Software*, 51, 1–25. <https://doi.org/10.18637/jss.v051.i12>.
- Therneau, T., and Atkinson, B. (2025), *Rpart: Recursive Partitioning and Regression Trees*. <https://doi.org/10.32614/CRAN.package.rpart>.
- Wickham, H. (2016), *ggplot2: Elegant graphics for data analysis*, Springer-Verlag New York.
- Wickham, H. (2022), *classify: Explore Classification Models in High Dimensions*. <https://doi.org/10.32614/CRAN.package.classify>.
- Wickham, H., Cook, D., and Hofmann, H. (2015), “Visualizing Statistical Models: Removing the Blindfold,” *Statistical Analysis and Data Mining: The ASA Data Science Journal*, Wiley Online Library, 8, 203–225. <https://doi.org/10.1002/sam.11271>.
- Wickham, H., Cook, D., Hofmann, H., Buja, A., and others (2011), “Tourr: An R Package for Exploring Multivariate Data with Projections,” *Journal of Statistical Software*, American Statistical Association, 40, 1–18. <https://doi.org/10.18637/jss.v040.i02>.

6.1 Appendix

Table 3: Source data information

Name	URL
data12	https://archive.ics.uci.edu/dataset/518/speaker+accent+recognition
data13-1	https://archive.ics.uci.edu/dataset/547/algerian+forest+fires+dataset
data13-2	https://archive.ics.uci.edu/dataset/547/algerian+forest+fires+dataset
data20-1	https://archive.ics.uci.edu/dataset/357/occupancy+detection
data20-2	https://archive.ics.uci.edu/dataset/357/occupancy+detection
data20-3	https://archive.ics.uci.edu/dataset/357/occupancy+detection
data21	https://archive.ics.uci.edu/dataset/537/cervical+cancer+behavior+risk
data22-1	https://archive.ics.uci.edu/dataset/257/user+knowledge+modeling
data22-2	https://archive.ics.uci.edu/dataset/257/user+knowledge+modeling
data26	https://archive.ics.uci.edu/dataset/308/gas+sensor+array+under+flow+modulation
data27-a11	https://archive.ics.uci.edu/dataset/302/gesture+phase+segmentation
data27-a21	https://archive.ics.uci.edu/dataset/302/gesture+phase+segmentation
data27-a31	https://archive.ics.uci.edu/dataset/302/gesture+phase+segmentation
data27-a32	https://archive.ics.uci.edu/dataset/302/gesture+phase+segmentation
data27-b11	https://archive.ics.uci.edu/dataset/302/gesture+phase+segmentation
data27-b12	https://archive.ics.uci.edu/dataset/302/gesture+phase+segmentation
data27-b31	https://archive.ics.uci.edu/dataset/302/gesture+phase+segmentation
data27-b32	https://archive.ics.uci.edu/dataset/302/gesture+phase+segmentation
data27-c11	https://archive.ics.uci.edu/dataset/302/gesture+phase+segmentation
data27-c12	https://archive.ics.uci.edu/dataset/302/gesture+phase+segmentation
data27-c31	https://archive.ics.uci.edu/dataset/302/gesture+phase+segmentation
data27-c32	https://archive.ics.uci.edu/dataset/302/gesture+phase+segmentation
data29	https://archive.ics.uci.edu/dataset/282/lsvt+voice+rehabilitation
data32	https://archive.ics.uci.edu/dataset/257/user+knowledge+modeling
data34	https://archive.ics.uci.edu/dataset/267/banknote+authentication
data36	https://archive.ics.uci.edu/dataset/236/seeds
data37-1	https://archive.ics.uci.edu/dataset/231/pamap2+physical+activity+monitoring
data37-2	https://archive.ics.uci.edu/dataset/231/pamap2+physical+activity+monitoring
data37-3	https://archive.ics.uci.edu/dataset/231/pamap2+physical+activity+monitoring
data37-4	https://archive.ics.uci.edu/dataset/231/pamap2+physical+activity+monitoring
data37-5	https://archive.ics.uci.edu/dataset/231/pamap2+physical+activity+monitoring
data37-8	https://archive.ics.uci.edu/dataset/231/pamap2+physical+activity+monitoring
data37-14	https://archive.ics.uci.edu/dataset/231/pamap2+physical+activity+monitoring
data38	https://archive.ics.uci.edu/dataset/230/planning+relax
data39-1	https://archive.ics.uci.edu/dataset/224/gas+sensor+array+drift+dataset

data39-2 <https://archive.ics.uci.edu/dataset/224/gas+sensor+array+drift+dataset>
 data39-3 <https://archive.ics.uci.edu/dataset/224/gas+sensor+array+drift+dataset>
 data39-4 <https://archive.ics.uci.edu/dataset/224/gas+sensor+array+drift+dataset>
 data39-5 <https://archive.ics.uci.edu/dataset/224/gas+sensor+array+drift+dataset>
 data39-6 <https://archive.ics.uci.edu/dataset/224/gas+sensor+array+drift+dataset>
 data39-7 <https://archive.ics.uci.edu/dataset/224/gas+sensor+array+drift+dataset>
 data39-8 <https://archive.ics.uci.edu/dataset/225/gas+sensor+array+drift+dataset>
 data39-9 <https://archive.ics.uci.edu/dataset/226/gas+sensor+array+drift+dataset>
 data41-1 <https://archive.ics.uci.edu/dataset/194/wall+following+robot+navigation+data>
 data41-2 <https://archive.ics.uci.edu/dataset/194/wall+following+robot+navigation+data>
 data41-3 <https://archive.ics.uci.edu/dataset/194/wall+following+robot+navigation+data>
 data42 <https://archive.ics.uci.edu/dataset/192/breast+tissue>
 data44 <https://archive.ics.uci.edu/dataset/181/libras+movement>
 data49-2 <https://archive.ics.uci.edu/dataset/167/hill+valley>
 data49-3 <https://archive.ics.uci.edu/dataset/168/hill+valley>
 data49-4 <https://archive.ics.uci.edu/dataset/169/hill+valley>
 data50 <https://archive.ics.uci.edu/dataset/161/mammographic+mass>
 data52-1 <https://archive.ics.uci.edu/dataset/96/spectf+heart>
 data52-2 <https://archive.ics.uci.edu/dataset/96/spectf+heart>
 data53 <https://archive.ics.uci.edu/dataset/139/synthetic+control+chart+time+series>
 data55-1 <https://archive.ics.uci.edu/dataset/80/optical+recognition+of+handwritten+digits>
 data55-2 <https://archive.ics.uci.edu/dataset/80/optical+recognition+of+handwritten+digits>
 data56-1 <https://archive.ics.uci.edu/dataset/81/pen+based+recognition+of+handwritten+digits>
 data56-2 <https://archive.ics.uci.edu/dataset/81/pen+based+recognition+of+handwritten+digits>
 data57 <https://archive.ics.uci.edu/dataset/39/ecoli>
 data61-1 <https://archive.ics.uci.edu/dataset/54/isolet>
 data62 <https://archive.ics.uci.edu/dataset/74/musk+version+1>
 data63 <https://archive.ics.uci.edu/dataset/75/musk+version+2>
 data64-1 <https://archive.ics.uci.edu/dataset/146/statlog+landsat+satellite>
 data64-2 <https://archive.ics.uci.edu/dataset/146/statlog+landsat+satellite>
 data65 <https://archive.ics.uci.edu/dataset/15/breast+cancer+wisconsin+original>
 data66 <https://archive.ics.uci.edu/dataset/62/lung+cancer>
 data67 <https://archive.ics.uci.edu/dataset/59/letter+recognition>
 data68-1 <https://archive.ics.uci.edu/dataset/50/image+segmentation>
 data68-2 <https://archive.ics.uci.edu/dataset/50/image+segmentation>
 data69-1 <https://archive.ics.uci.edu/dataset/107/waveform+database+generator+version+1>
 data69-2 <https://archive.ics.uci.edu/dataset/107/waveform+database+generator+version+1>
 data70 <https://archive.ics.uci.edu/dataset/42/glass+identification>
 data71-1 <https://archive.ics.uci.edu/dataset/148/statlog+shuttle>
 data71-2 <https://archive.ics.uci.edu/dataset/148/statlog+shuttle>
 data72-1 <https://archive.ics.uci.edu/dataset/149/statlog+vehicle+silhouettes>

data72-2	https://archive.ics.uci.edu/dataset/149/statlog+vehicle+silhouettes
data72-3	https://archive.ics.uci.edu/dataset/149/statlog+vehicle+silhouettes
data72-4	https://archive.ics.uci.edu/dataset/149/statlog+vehicle+silhouettes
data72-5	https://archive.ics.uci.edu/dataset/149/statlog+vehicle+silhouettes
data72-6	https://archive.ics.uci.edu/dataset/149/statlog+vehicle+silhouettes
data72-7	https://archive.ics.uci.edu/dataset/149/statlog+vehicle+silhouettes
data73	https://archive.ics.uci.edu/dataset/151/connectionist+bench+sonar+mines+vs+rocks
data74	https://archive.ics.uci.edu/dataset/152/connectionist+bench+vowel+recognition+deterdin
NCI60	https://github.com/natydasilva/PPforest/blob/master/data/NCI60.rda
crab	https://github.com/natydasilva/PPforest/blob/master/data/crab.rda
fishcatch	https://github.com/natydasilva/PPforest/blob/master/data/fishcatch.rda
glass	https://github.com/natydasilva/PPforest/blob/master/data/glass.rda
image	https://github.com/natydasilva/PPforest/blob/master/data/image.rda
leukemia	https://github.com/natydasilva/PPforest/blob/master/data/leukemia.rda
lymphoma	https://github.com/natydasilva/PPforest/blob/master/data/lymphoma.rda
olive	https://github.com/natydasilva/PPforest/blob/master/data/olive.rda
parkinson	https://github.com/natydasilva/PPforest/blob/master/data/parkinson.rda
wine	https://github.com/natydasilva/PPforest/blob/master/data/wine.rda

Table 4: Overview of benchmark datasets

dataset	Cases	Predictors	Groups	Imbalance	Correlation
data12	329	12	6	0.41	0.38
data13-1	122	13	2	0.03	0.41
data13-2	121	13	2	0.29	0.37
data20-1	2665	5	2	0.27	0.81
data20-2	9752	5	2	0.58	0.29
data20-3	8143	5	2	0.58	0.45
data21	72	19	2	0.42	0.22
data22-1	258	5	4	0.25	0.12
data22-2	145	5	4	0.14	0.18
data26	58	435	4	0.21	0.64
data27-a11	1747	18	5	0.38	0.24
data27-a21	1264	18	5	0.35	0.22
data27-a31	1834	18	5	0.28	0.27
data27-a32	1830	32	5	0.28	0.13
data27-b11	1072	18	5	0.31	0.27
data27-b12	1069	32	5	0.32	0.13
data27-b31	1424	18	5	0.21	0.24

data27-b32	1420	32	5	0.21	0.11
data27-c11	1111	18	5	0.14	0.27
data27-c12	1107	32	5	0.13	0.11
data27-c31	1448	18	5	0.17	0.27
data27-c32	1444	32	5	0.17	0.11
data29	126	310	2	0.33	0.28
data32	403	6	4	0.20	0.11
data34	1372	4	2	0.11	0.43
data36	210	7	3	0.00	0.61
data37-1	29101	53	5	0.23	0.17
data37-14	769	53	2	0.52	0.16
data37-2	14132	53	3	0.62	0.18
data37-3	11835	53	4	0.34	0.16
data37-4	16357	53	5	0.29	0.15
data37-5	17560	53	5	0.21	0.16
data37-8	22990	53	9	0.27	0.17
data38	182	12	2	0.43	0.21
data39-1	445	128	6	0.15	0.55
data39-2	1239	128	5	0.35	0.40
data39-3	1586	128	5	0.17	0.56
data39-4	161	128	5	0.32	0.43
data39-5	197	128	5	0.22	0.57
data39-6	2300	128	6	0.25	0.61
data39-7	3613	128	6	0.11	0.68
data39-8	294	128	6	0.43	0.57
data39-9	470	128	6	0.10	0.42
data41-1	5456	2	4	0.34	0.03
data41-2	5456	4	4	0.34	0.15
data41-3	5456	24	4	0.34	0.17
data42	106	9	6	0.08	0.51
data44	360	90	15	0.00	0.27
data49-2	606	100	2	0.03	1.00
data49-3	606	100	2	0.01	0.99
data49-4	606	100	2	0.01	0.99
data50	830	5	2	0.03	0.23
data52-1	80	44	2	0.00	0.25
data52-2	187	44	2	0.84	0.29
data53	600	60	6	0.00	0.46
data55-1	3823	64	10	0.00	0.12
data55-2	1797	64	10	0.01	0.12
data56-1	7494	16	10	0.01	0.27

data56-2	3498	16	10	0.01	0.28
data57	327	7	5	0.38	0.23
data61-1	6238	617	26	0.00	0.17
data62	476	166	2	0.13	0.26
data63	6598	166	2	0.69	0.27
data64-1	4435	36	6	0.15	0.49
data64-2	2000	36	6	0.13	0.50
data65	683	9	2	0.30	0.60
data66	27	56	3	0.07	0.20
data67	20000	16	26	0.00	0.18
data68-1	210	19	7	0.00	0.30
data68-2	2100	19	7	0.00	0.28
data69-1	5000	21	3	0.01	0.30
data69-2	5000	40	3	0.01	0.09
data70	214	9	6	0.31	0.23
data71-1	43500	9	7	0.78	0.19
data71-2	14494	9	5	0.79	0.20
data72-1	94	18	4	0.09	0.39
data72-2	94	18	4	0.05	0.40
data72-3	94	18	4	0.10	0.42
data72-4	94	18	4	0.12	0.42
data72-5	94	18	4	0.10	0.49
data72-6	94	18	4	0.06	0.40
data72-7	94	18	4	0.06	0.44
data73	208	60	2	0.07	0.23
data74	990	12	11	0.00	0.22
NCI60	56	31	7	0.05	0.56
crab	200	6	4	0.00	0.95
fishcatch	159	7	7	0.31	0.46
glass	214	10	6	0.31	0.23
image	2310	19	7	0.00	0.28
leukemia	72	41	3	0.40	0.44
lymphoma	80	51	3	0.41	0.75
olive	572	9	9	0.32	0.35
parkinson	195	23	2	0.51	0.50
wine	178	14	3	0.13	0.30

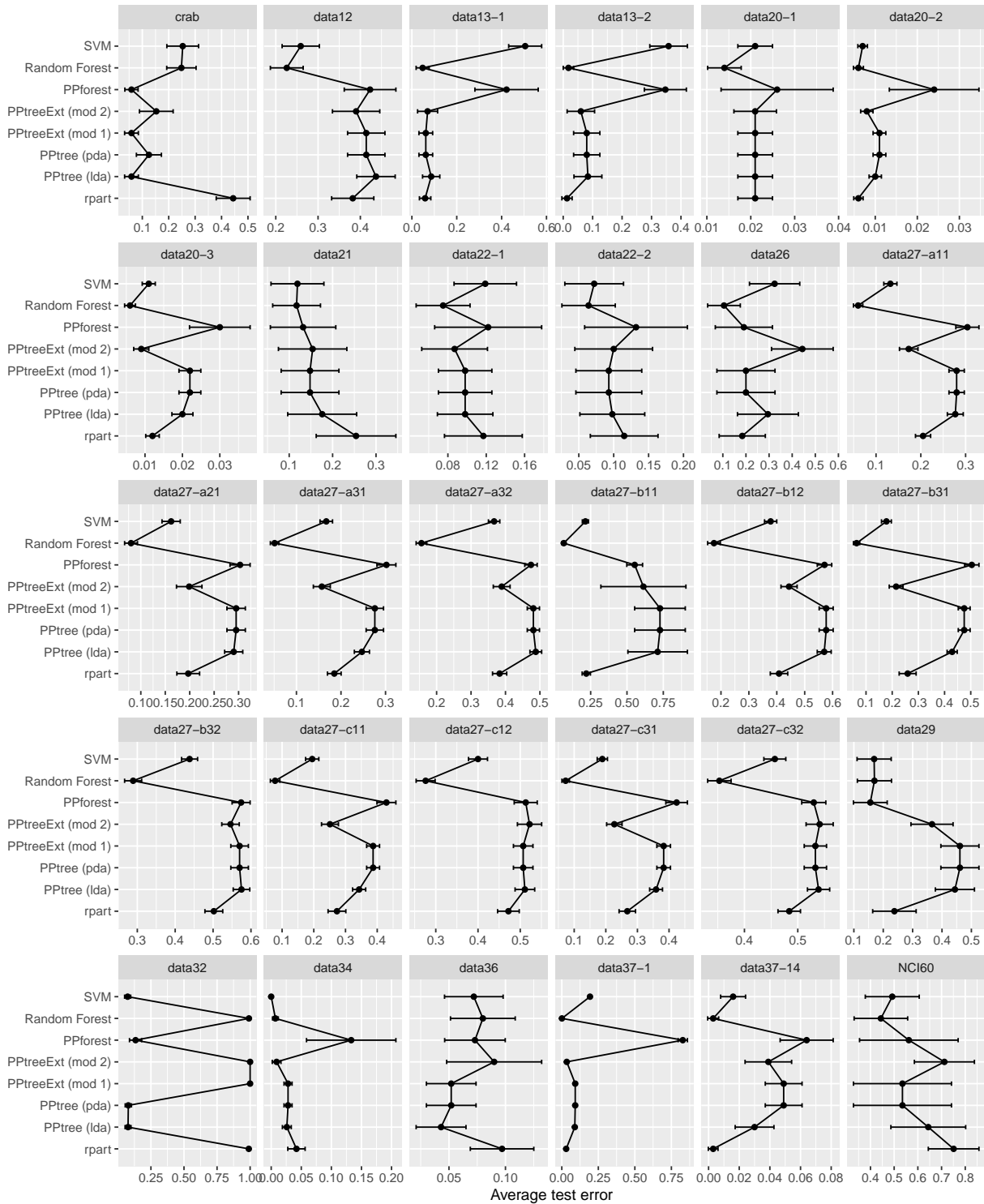


Figure 12: Average test error from 200 training/test splits of benchmark data for: SVM, Random Forest, PPtree (pda), PPtree (LDA), PPtreeExt modifications 1 and 2, PPforest and rpart.

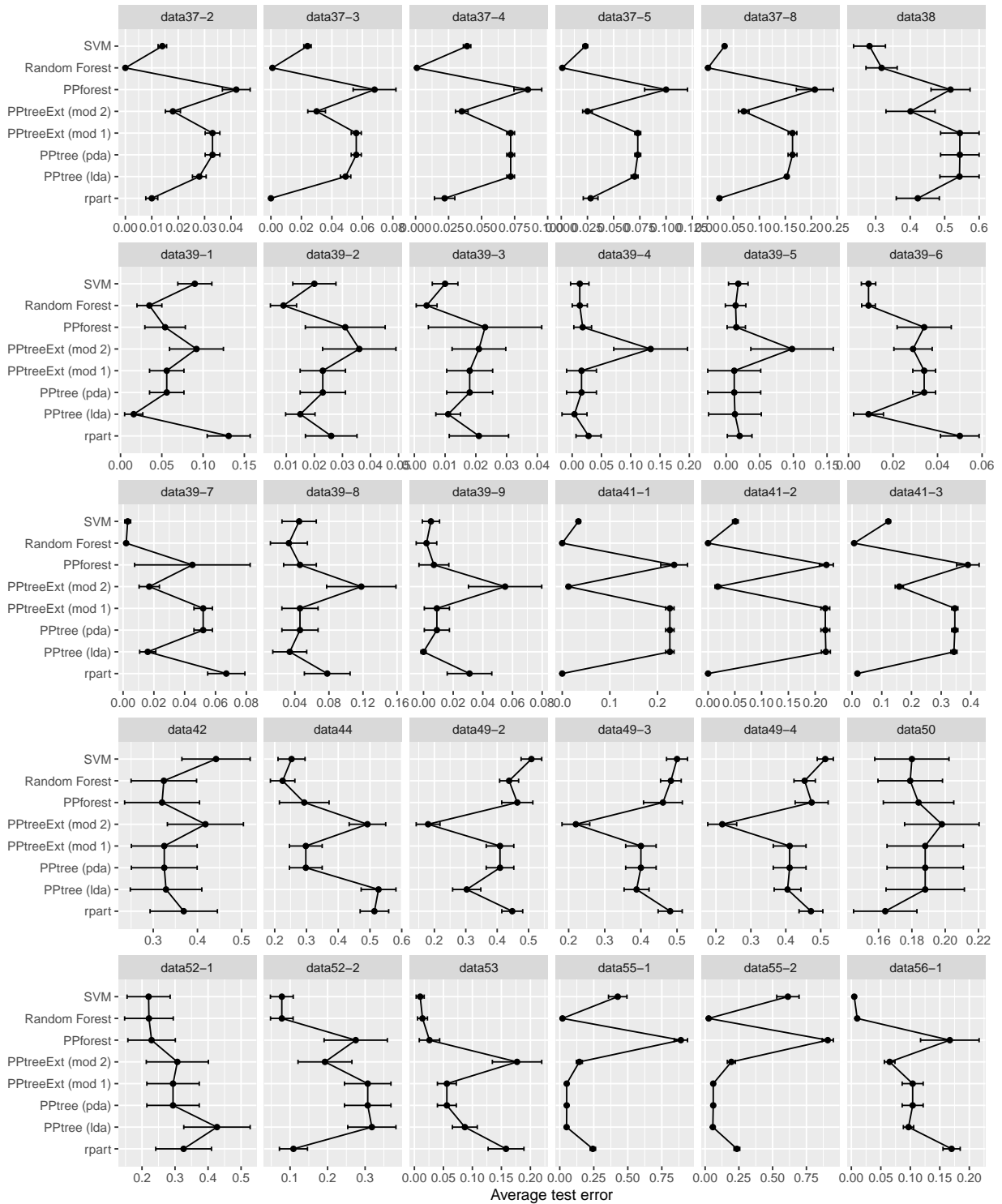


Figure 13: Average test error from 200 training/test splits of benchmark data for: SVM, Random Forest, PPtree (pda), PPtree (LDA), PPtreeExt modifications 1 and 2, PPforest and rpart.

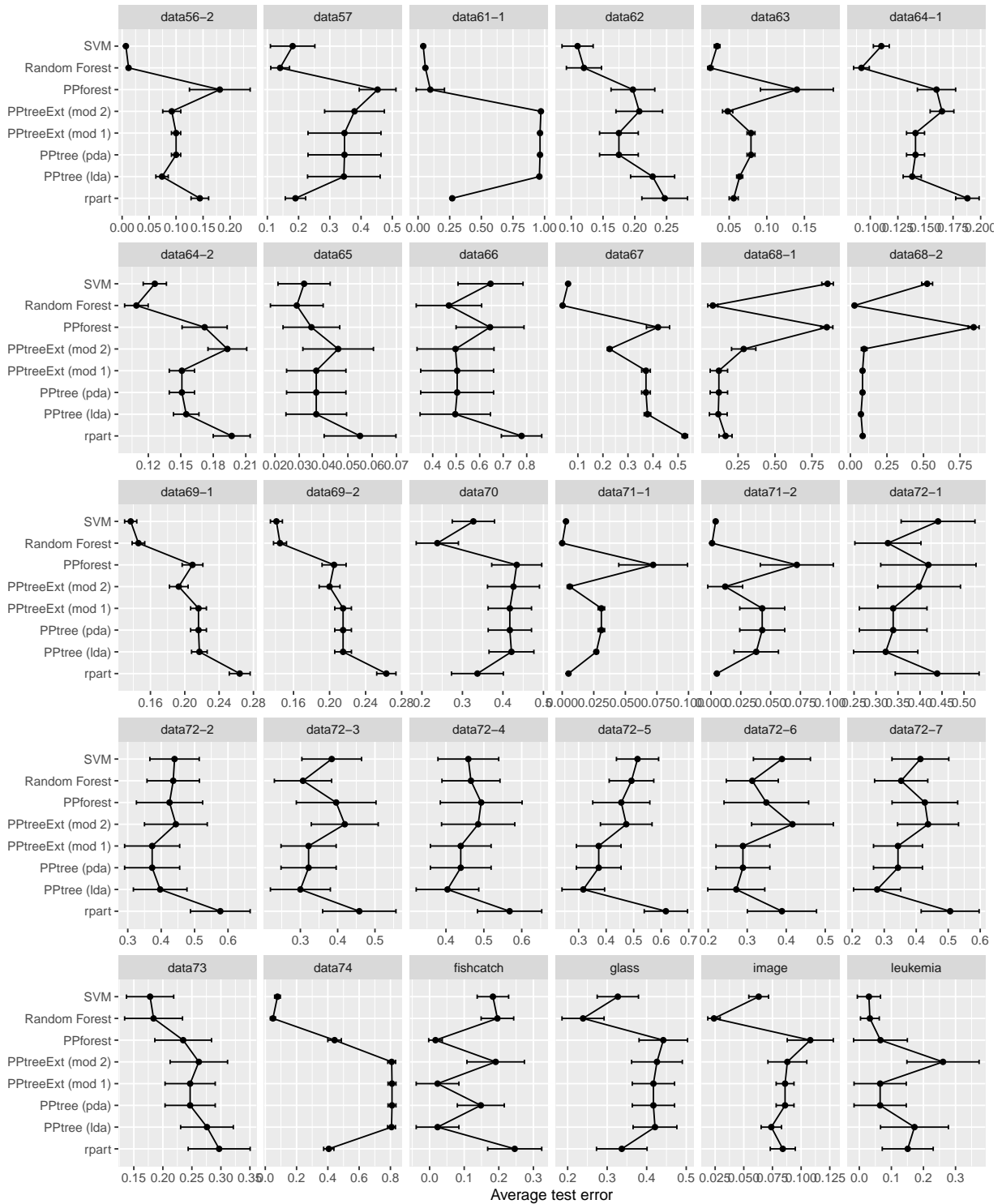


Figure 14: Average test error from 200 training/test splits of benchmark data for: SVM, Random Forest, PPtree (pda), PPtree (LDA), PPtreeExt modifications 1 and 2, PPforest and rpart.

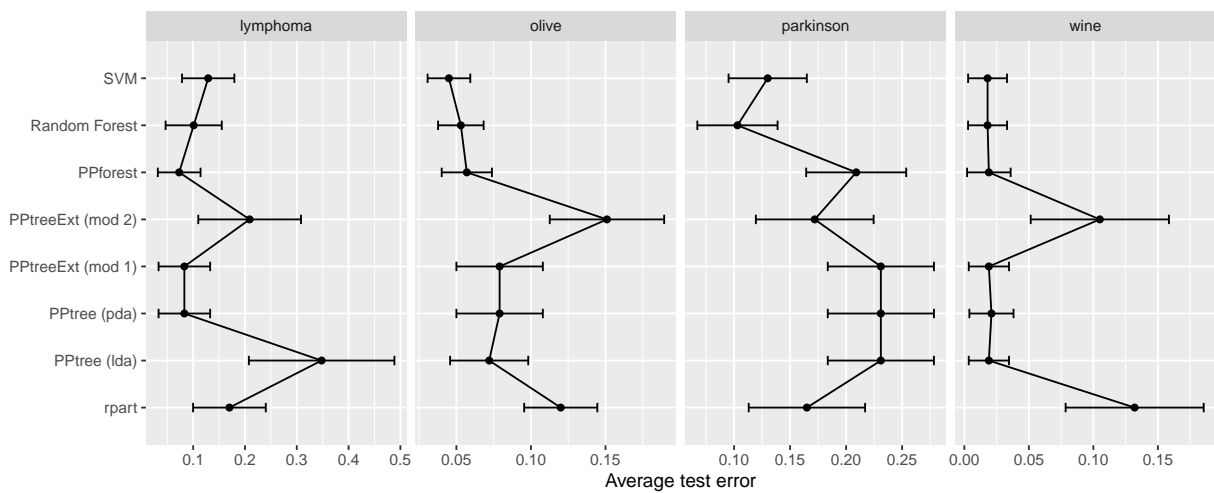


Figure 15: Average test error from 200 training/test splits of benchmark data for: SVM, Random Forest, PPtree (pda), PPtree (LDA), PPtreeExt modifications 1 and 2, PPforest and rpart.